JMEPEG (2012) 21:2559–2565
DOI: 10.1007/s11665-012-0302-4

1059-9495/$19.00

Effect of Annealing and Cold Work on Mechanical Properties of Beta III Titanium

S. Cai, D.M. Bailey, and L.E. Kay

(Submitted February 13, 2012; in revised form June 25, 2012)

Experiments have been carried out to study the effect of annealing and cold work (CW) on the mechanical properties of beta III Ti alloy. Material was annealed at different temperatures above the beta transformation temperature, and then cold drawn to about 53% area reduction. Cyclic tensile test was performed to study the evolution of mechanical properties and the recoverable strain during process. Results show that the effect of annealing and CW is closely related to the stress-induced martensite (SIM) phase transformation. Lower annealing temperature results in higher strength and recoverable strain, which is further increased by CW. A total recoverable strain of ~3.2% was obtained from the annealed and CW sample.

Keywords beta III titanium, recoverable strain, stress-induced martensite transformation, superelastic strain

1. Introduction

Stainless steels and nickel titanium alloys (e.g., nitinol) are two common metal materials used in medical applications such as orthodontic archwire and intravascular guide wire. However, the relatively low spring-back or recoverable strain of stainless steels and the relatively low stiffness of nickel titanium alloys raises the interest of the medical industry in searching for materials that have better spring-back, torsion, and stiffness properties (Ref 1, 2). For applications such as the intravascular guidewire, large spring-back is critical for the material to pass through the complicated blood pathway without damaging the tissue, while high stiffness provides good torsion and push-ability that helps the material to be inserted close to the end of the blood vessel. Interest has been focused on β titanium alloys, which have large recoverable strains due to stress-induced martensite (SIM) during deformation (Ref 3-7). Among β Ti alloys, beta III Ti is widely used in medical applications such as the orthodontic archwire (Ref 1) and recently the intravascular guidewire (Ref 2). Figure 1 compares stress strain curve of our standard straight annealed beta III Ti wire with those of 316 stainless steel and nitinol wires. It shows that beta III Ti has mechanical properties between those two alloys, indicating a great potential for this material in the medical industry. However, it can be seen that the recoverable strain of beta III Ti is still very low compared to that of nitinol (e.g., ~2.2% recoverable strain of beta III vs. a full recovery of nitinol at 4% strain, and it is known that the maximum recovery strain of nitinol can reach ~11% under certain condition). Previous studies of Laheurte et al. (Ref 7, 8) on this material reported a maximum recoverable strain of above 4% after pre-straining a large grain sized wire. According to them, the recoverable strain increases with increasing grain size. To the authors' knowledge, this is the only published research on superelasticity of beta III Ti alloy. Clearly, more studies are needed. In this article, we reported our recent experiments on the influences of annealing and cold work (CW) on mechanical properties, particularly the recoverable strain, of beta III Ti alloy. Recently, we have seen an increasing interest from the medical industry on this material. This work will benefit the industries and help to produce better products.

2. Material and Experiments

The material used in this study is Ti-10.92 wt.% Mo-6.23 wt.% Zr-4.53 wt.% Sn-0.02 wt.% Fe-0.1 wt.% O and <0.01 wt.% N and H. The original material was a cold drawn wire with ~50% CW. The wire diameter is ~1.5 mm. This material was then strand annealed at temperatures range from 816 to 1093 °C, which are above its β-transus temperature (~760 °C), in an argon filled atmosphere. The speed was set up such that the wire passed through the hot zone in ~1.5 min. Wires were quenched by pressurized argon gas. Samples were polished and etched by Kroll's Reagent to reveal the microstructures after anneal. Microstructures were analyzed at Fort Wayne Metals' Material Lab (Fort Wayne, IN) and Materials Evaluation and Engineering, Inc (MEE, Plymouth, MN). The grain size was determined per ASTM E 112 using the Abrams three-circle procedure. About 5-8 areas were evaluated for each sample dependent on the grain size. Tensile test was carried out on an Instron tensile tester with load cells that have capacities range from 1 to 10 kN. During the test, the samples was first pulled to 4% strain and unloaded at a strain rate of 0.01 per minute. Once the load reached zero, the sample was re-loaded and pulled to fracture in a strain rate of 0.07 per minute. The

This article is an invited paper selected from presentations at the International Conference on Shape Memory and Superelastic Technologies 2011, held November 6-9, 2011, in Hong Kong, China, and has been expanded from the original presentation.

S. Cai, D.M. Bailey, and **L.E. Kay**, Fort Wayne Metals Research Products Corporation, Fort Wayne, IN 46809. Contact e-mail: song_cai@fwmetals.com.

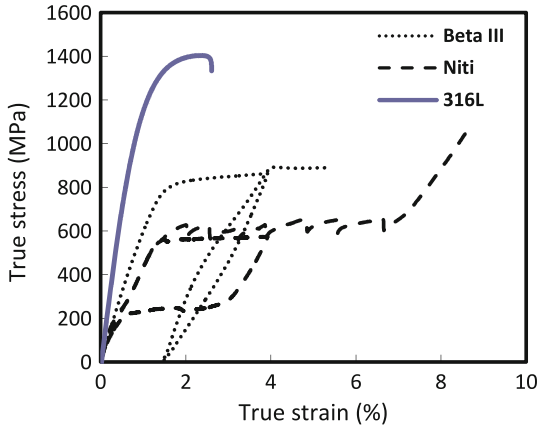

Fig. 1 Stress strain curves of the beta III titanium after straight anneal, 316L stainless steel in spring condition and nitinol in super-elastic condition

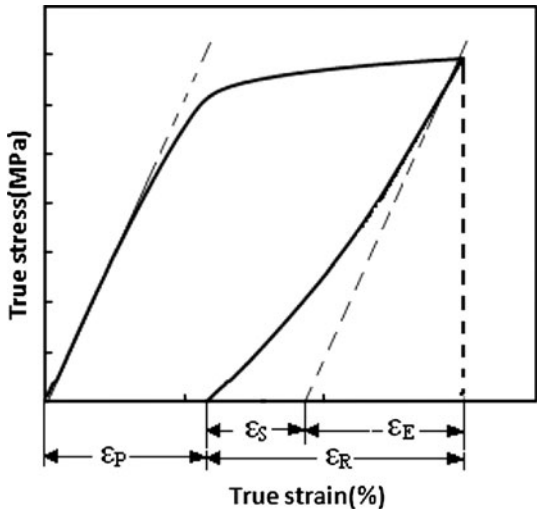

Fig. 2 Schematic illustrates the applied and recoverable strains. ε_P is the plastic strain, ε_R is the total recoverable strain after unload at the test temperature. It includes the elastic strain, ε_E, and the reversal phase transformation strain, ε_S

gage length is 254 mm. The deformation strain was determined based on the displacement of the Instron crosshead. 2-3 samples were tested for each data point. The total recoverable strain, elastic strain, and the reversal phase transformation strain (which is called super-elastic strain hereafter) were obtained from the stress strain curve as illustrated in Fig. 2. The yield strength (YS) was determined by the 0.2% offset method.

All the annealed wires were then cold drawn four times at a diameter of ~1.0 mm corresponding to a 53% CW reduction. Each pass has a CW reduction ~10-20%. The evolution of mechanical properties was tracked after each drawing step using the same test method described above. All tests were carried out at room temperature.

X-ray diffraction was carried out on an APD 3520 x-ray diffractometer with Cu Kα radiation to identify the phases presented after anneal and deformation. The accelerating voltage is at 40 kV and current is at 30 mA. The scan step size is 0.005° and the counting time is 0.2-0.25 s per step.

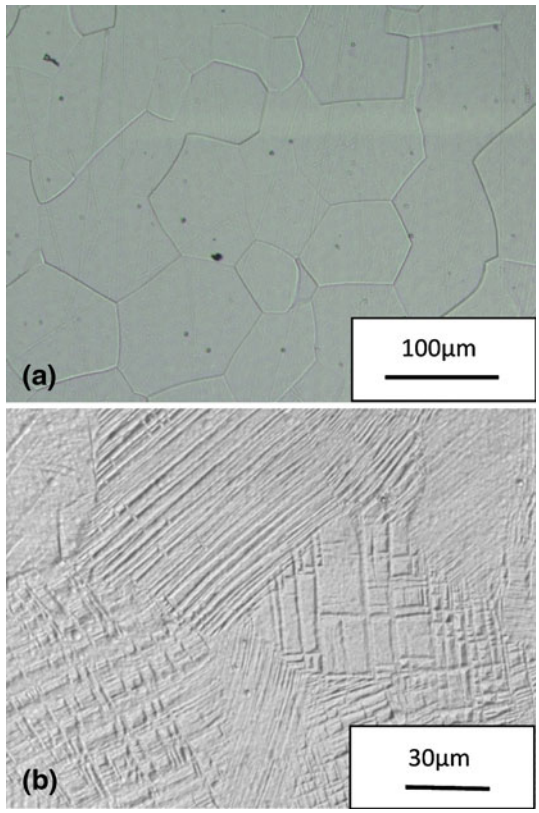

Fig. 3 Microstructures after (a) solution treated at 1093 °C shows an equiaxed grain structure and (b) solution treated at 1093 °C followed by 16% CW shows a deformation structure

Table 1 Grain size (μm) after annealed at different temperatures

816 °C	871 °C	927 °C	982 °C	1038 °C	1093 °C
11 ± 1.3	22 ± 2.6	30.0 ± 3.6	40.2 ± 3.7	60.7 ± 7.3	84.4 ± 8.3

3. Experimental Results

3.1 Microstructures

After anneal at temperatures from 816 to 1093 °C, all samples have a recrystallized microstructure as illustrated in Fig. 3(a). The average grain sizes are listed in Table 1. It is seen that grain size increases with increasing annealing temperature. X-ray diffraction spectrum of materials annealed at 816 to 1093 °C in Fig. 4 shows that after anneal, materials consist of single β-phase, no obvious α-phase or ω-phase peaks can be observed. Figure 3(b) shows the microstructure after 16% CW, where the striations of mechanical twinning or SIM can be seen. The presence of SIM in the deformed sample is confirmed by the additional peaks in the x-ray diffraction spectrum, as shown in Fig. 4.

3.2 Mechanical Properties

The mechanical properties after annealing at various temperatures are plotted in Fig. 5. It can be seen that both the YS and ultimate tensile strength (UTS) decreased with increasing

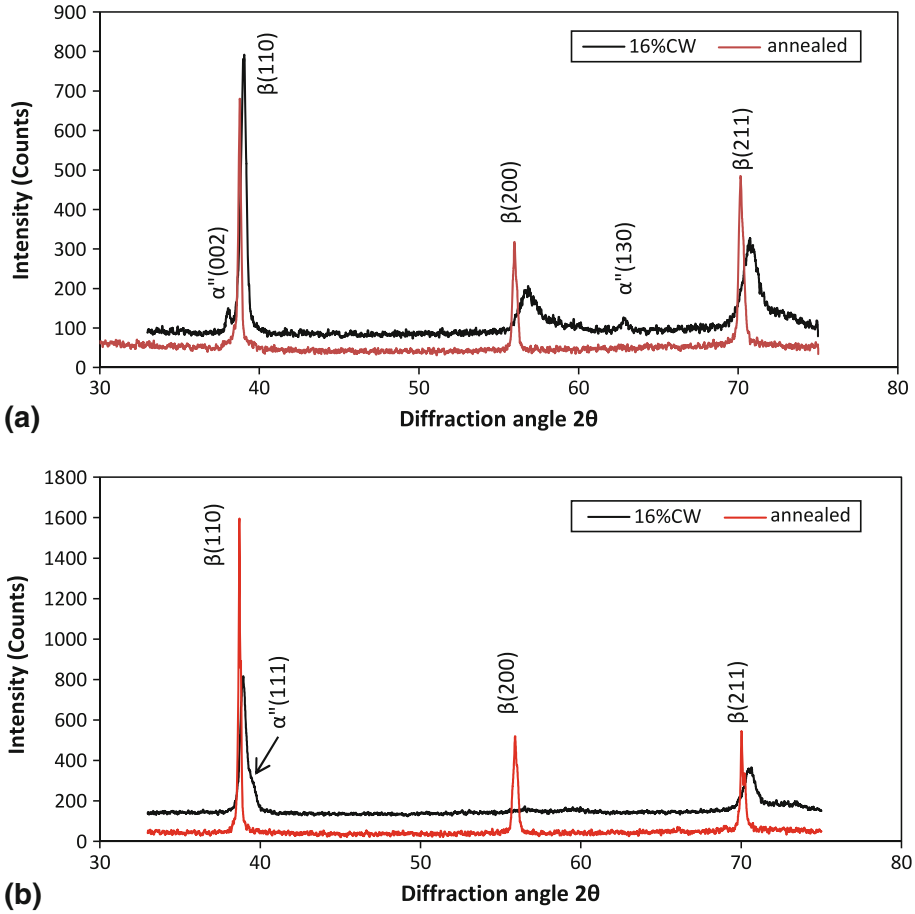

Fig. 4 X-ray diffraction profile of materials annealed at (a) 816 °C and (b) 1093 °C. The upper line in each plot represents the deformed material, the lower line represents the annealed material. d-Spacing of α″ martensite was calculated using the lattice parameters in Ref 17

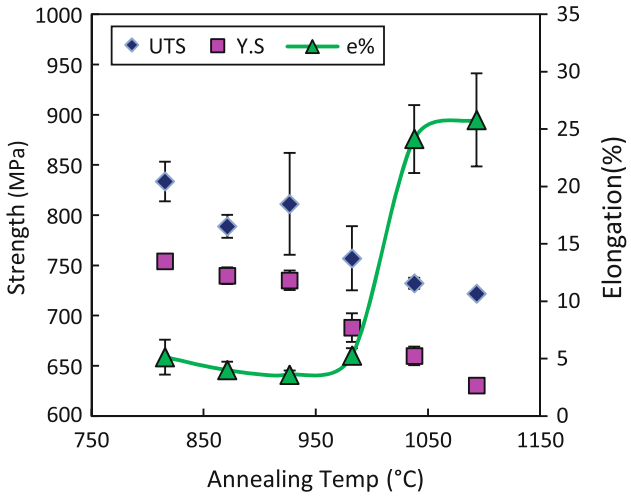

Fig. 5 Mechanical properties after annealed at different temperatures

annealing temperature. While the total elongation (e %) did not change until the annealing temperature raised to above 1000 °C, where an e % larger than 20% was obtained. The Young's modulus of all the annealed samples was very close to each other with an average value of 57.8 ± 0.8 GPa.

Figure 6(a) shows that the Young's modulus was independent to the annealing temperature, but decreased by CW. Young's modulus was decreased by ~10 GPa to about 47 GPa after the first drawing pass. After that, very small change was observed with further increasing CW reduction. The Young's modulus after 53% CW was ~48 GPa for all samples. The YSs of all annealed samples first decreased and reached a minimum value after 16% CW, after that they increased with increasing CW in a near linear relationship (Fig. 6b). On the contrary, UTSs continuously increased with CW, as shown in Fig. 6(c).

3.3 Recoverable Strain

Figure 7(a) shows the effect of changing annealing temperature on the recoverable strain, it can be seen that lower annealing temperature results in higher recoverable strain. At 4% deformation strain, the total recoverable strain was ~2.5% for sample annealed at 816 °C, and it decreased to ~2% as the annealing temperature increased to 1093 °C. However, these differences disappeared after CW (Fig. 7b); all samples that were annealed at different temperatures had recoverable strain of ~2.7% after 16% CW. Increasing the amount of CW increased recoverable strain. After 53% CW, all samples had recoverable strain of ~3.2%, corresponding to an approximate 80% strain recovery after unloading from 4% tensile strain.

Figure 8(a) shows that the elastic strain, ε_E, increased with increasing CW to ~40% reduction. Further increasing CW did not produce big change in elastic strain. On the contrary, Fig. 8(b) shows that super-elastic strain, ε_S, was decreased by CW to ~40% reduction. From Fig. 8(b), it can be seen that

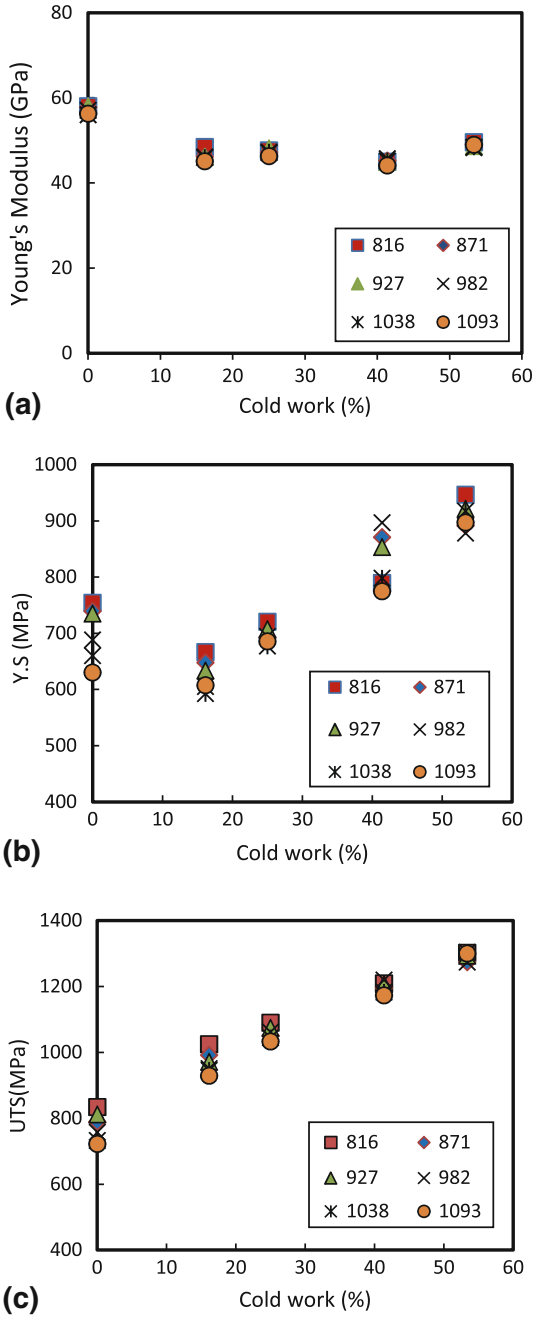

Fig. 6 Effects of CW on (a) Young's modulus, (b) YS, and (c) tensile strength. The standard deviation in (a) varies from 0.3 to 3 GPa. The deviation in (b) varies from 3 to 40 MPa in (b) and from 1 to 50 MPa in (c)

samples annealed at lower temperature have larger super-elastic strain, ε_S. The maximum ε_S of ~1% was obtained after anneal at 816 °C. It is also worthy to note that all samples have the similar ε_S once CW was put into the material.

4. Discussions

4.1 Effect of Annealing and CW on Mechanical Properties

The reason for the decreased mechanical strength with increasing annealing temperature appears to be obvious as the

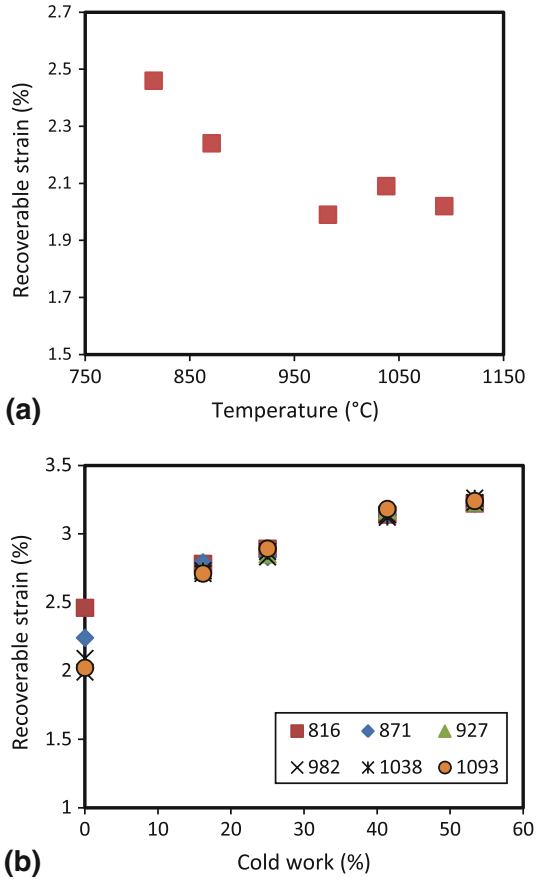

Fig. 7 Recoverable strains after annealed at different temperatures (a) and after different amounts of CW (b)

grain size increased with increasing annealing temperature. However, the jump in elongation at temperatures ~1000 °C is hard to explain. One may think that there might be some ω or α precipitates in the material before anneal, and since the annealing time is very short (i.e., only ~1.5 m in hot zone), these precipitates may remain in the matrix after annealed at lower temperature, but may be dissolved after annealed at higher temperatures. This explanation, however, is unlikely as the x-ray did not show any diffraction peaks from both phases in the annealed condition (Fig. 4). One possible reason is that after annealing at different temperatures, different texture orientations were produced. In other words, after annealed at low temperatures, the material may still maintain the deformation texture, while a full recrystallization texture may be developed after high temperature anneal. Different textures could affect the deformation modes and result in different ductilities. For an example, for a material with a random texture, once grains with a preferred orientation yield (e.g., grains with the {110} plane in the loading direction), load will be transferred to their neighboring grains, which are still in the elastic deformation region due to their different orientations (e.g., grains with the {200} plane in the loading direction). This load transfer between different crystal orientations results in high work hardening rate and thus longer elongation. On the other hand, for a material with strong texture, since most of the grains aligned in the similar direction, the effect of load partitioning is limited. Therefore, once yield happens, local deformation will be quickly developed and results in lower

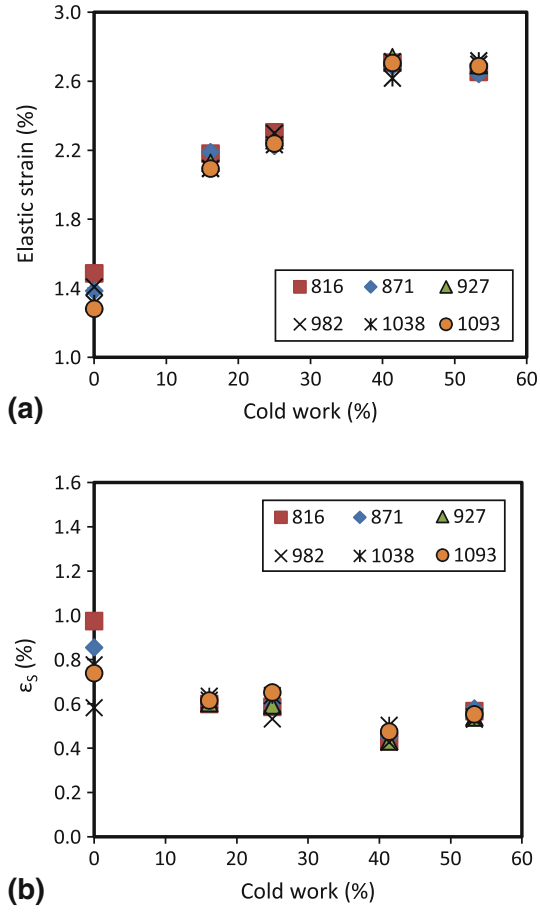

Fig. 8 (a) Elastic strain and (b) superelastic strain

elongation. However, since texture measurement has not been carried at this moment, this possibility has not been confirmed and requires further study.

The decrease in Young's modulus by the cold drawing process can be explained by the formation of SIM as it has been found to have the lowest modulus among all the phases in β Ti system (Ref 9). Similar behavior has been observed in other β Ti alloys (Ref 10, 11) and other materials, such as 304 stainless steel (Ref 12) and nitinol (Ref 13), that involve SIM during deformation. In Ref 14, Shastry et al. studied the influence of CW to mechanical properties of beta III Ti and obtained a Young's modulus of about 55 GPa, which is very close to our result for the annealed sample. However, they reported that the Young's modulus continuously increased by CW, which is in contrast to our observation. The Young's modulus of the annealed sample was, however, not reported in their article (see Fig. 2 in Ref 14), thus it is not clear if the Young's modulus was decreased by CW at the beginning. It is interesting to note that their results on a beta Ti-13V-11Cr-3Al alloy (Fig. 1 in Ref 14), which included the annealed Young's modulus) did show a drop in Young's modulus after ~12% CW.

After the first drawing pass, the Young's modulus did not change too much with further increasing the amount of CW (Fig. 6a). This suggests that SIM has reached its maximum volume fraction after a small amount of CW (e.g., 16% CW).

Similarly, the decrease in YS caused by CW can be explained by SIM. As discussed in Ref 9, 15, martensite has lower YS than austenite. Therefore, the retained martensite (by pinning effects from dislocation or twinning) after CW reduced the YS of the bulk material. Since the deformation of beta III Ti is a combination of dislocation slip, mechanical twinning (both increase the YS), and SIM (Ref 16-18), the decrease in YS indicates that the effect of SIM is larger than that of the dislocation slip and twinning at the early stage of deformation. Since no more SIM was produced after the first drawing pass, the effect of SIM was surpassed by that of dislocation and twinning; therefore, the YS increased with increasing CW simply due to the work hardening effect of slip and twinning.

Compared to the YS, the UTS was increased by CW without a decrease at 16% CW, suggesting that SIM only has a significant influence on the early stage of deformation such as the elastic deformation and the elasto-plastic deformation, while dislocation slip and deformation twinning are the dominant deformation modes during the plastic deformation, which is consistent with the previous discussion.

4.2 Effect of Annealing and CW on Recoverable Strain

The effect of the annealing process on the recoverable strain of beta Ti alloys depends on the influences of microstructure and deformation modes. Any change that benefits the SIM and suppresses dislocation slip will improve the super-elastic strain. For example, annealing at intermediate temperatures (rather than solution treatment after CW), the retained work hardening or dislocation structures increases the critical stress for dislocation slip and promotes the nucleation of the SIM (Ref 19). This could explain the larger recoverable strain obtained after annealed at lower temperatures. In addition, studies of Kim et al. (Ref 19, 20) showed a strong texture dependence of the super-elastic strain, where the maximum recoverable strain was obtained in the ⟨110⟩ β-phase direction. Considering that bcc metals tend to form a ⟨110⟩ fiber texture during wire drawing (Ref 21), it is very likely that the larger recoverable strain obtained after lower temperature anneal (e.g., 816 °C) has benefited from the retained deformation texture. Increasing the annealing temperature resulted in the recrystallization texture, which might have reduced the ⟨110⟩ concentration in the wire axial direction and, therefore, decreased the recoverable strain. More studies regarding the texture evolution during annealing and its relationship to super-elasticity are recommended.

In their studies on the super-elasticity of the beta III Ti alloy, Laheurte et al. (Ref 7, 8) proposed that the recoverable strain increased with increasing grain size. However, our study shows an opposite sense, i.e., samples with smaller grains have larger recoverable strain than those with larger grains. This discrepancy is however not very surprising since previous studies on β Ti alloys have also found controversial influences of the grain size on SIM and the recoverable strain. Bhattacharjee et al. (Ref 22) studied a Ti-10V-2Fe-3Al beta alloy and observed an increased trigger stress for the SIM with increasing β-phase grain size. They proposed that the larger grain size resulted in higher elastic energy stored in the matrix during stress induced phase transformation, which delayed the SIM process. On the contrary, Grosdidier et al. (Ref 23) found that for the β-Cez Ti alloy (i.e., Ti-5Al-2Sn-2Cr-4Mo-4Zr-1Fe), the trigger stress for the SIM increased with decreasing grain size. They proposed that the strengthening of the matrix caused by grain refinement made it more difficult to accommodate the shape change of the martensite plate in the parent grain, and thus increased the stability of the parent phase. However, the study of Takashi

et al. (Ref 24) showed that the recoverable strain was independent of the β-phase grain size, but rather increased with decreasing quenching temperature. Miyazaki et al. (Ref 6) proposed that lower temperature annealing increased the critical stress for slip deformation and stabilized the super-elastic behavior due to the fine sub-grain structure and the high density of thermally re-arranged dislocations. The different results of the grain size effect between our research and those of Laheurte et al. (Ref 7, 8) are probably related to the differences during sample preparation and hence crystal textures. In Laheurte et al.'s study (Ref 7), the cold drawn wire has a rectangular shape, which likely has a somewhat different texture from our cold drawn round wire. Therefore, the textures after anneal are also likely different. Further in Ref (Ref 7), samples with the smaller grain size were prepared by annealing the cold drawn rectangular wire, while samples with the larger grain size were prepared by annealing the cold drawn rectangular wire, then cold rolling by 10% reduction and followed by a high temperature anneal. Hence, the textures in samples with different sizes will also likely be different. Even in Ref (Ref 7), the sample with large grain size does not always have a larger recoverable strain than that with smaller grain size (e.g., the one with grain size ~105 μm has a lower recoverable strain than that with grain size ~23 μm). One is thus led to doubt the conclusion of Lahuerte's statement about the grain size effect on the super-elastic strain. The experimental observations are likely the combined efforts of changes in both grain size and texture.

The influence of CW on super-elastic strain is two-fold. On one hand, CW raises the critical stress for twinning and slip and thus promotes SIM. In addition, dislocations and sub-grain boundaries produced by small pre-strain helps SIM by providing plastic accommodation for martensite shape strain (Ref 25) and acting as nucleation sites (Ref 26). On the other hand, too much dislocation or twins pin the grain boundaries and impedes the reversal phase transformation, and therefore reduce the super-elastic strain. In our case, the super-elastic strain slightly decreased with increasing CW (see Fig. 8b), indicating that the amount of CW range in this study might be too large, which produced a dislocation structure that retarded the reversal phase transformation and reduced the super-elastic strain. Future study will be focused on the influence of small pre-strain.

5. Conclusions

Experiments have been carried out to study the influences of annealing and CW on mechanical properties, especially the recoverable strain, of beta III Ti alloy. Following conclusions are obtained:

1. Mechanical strength of beta III Ti decreases with increasing annealing temperature following a near linear relationship, while the ductility largely increases when the annealing temperature is above 1000 °C.
2. The recoverable strain increases with decreasing annealing temperature.
3. CW decreases the Young's modulus and YS due to SIM.
4. CW increases the elastic strain, but slightly decreases the reversal phase transformation strain. The total recoverable strain increases with increasing CW. After unload from 4% tensile strain, a total recoverable strain of ~3.2% was obtained.

Acknowledgments

The authors would like to thank R. Gabet, A. Henry, J. Prascsak from Fort Wayne Metals and K. Schenk from Materials Evaluation and Engineering, Inc. for their help with the mechanical test and microstructure analysis. S. Cai also likes to thank Dr. Anne Argast from IPFW for the x-ray diffraction tests. Support from Fort Wayne Metals management on this project is greatly appreciated.

References

1. R.P. Kusy, A Review of Contemporary Archwires: Their Properties and Characteristics, *Angle Orthod.*, 1997, **67**(3), p 197–208
2. S. Nuss, Titanium Molybdenum Alloy Guidewire, US Patent No. 7,468,045, 2008
3. S. Hanada, M. Ozeki, and O. Izumi, Deformation Characteristics in Beta Phase Ti-Nb Alloys, *Metall. Trans.*, 1985, **16A**, p 789–795
4. S. Hanada, T. Yoshio, and O. Izumi, Effect of Plastic Deformation Modes on Tensile Properties of Beta Titanium Alloys, *Trans. Jpn. Inst. Met.*, 1986, **27**(7), p 496–503
5. E. Takahashi, T. Sakurai, S. Watanabe, N. Masahashi, and S. Hanada, Effect of Heat Treatment and Sn Content on Superelasticity in Biocompatible TiNbSn Alloys, *Mater. Trans.*, 2002, **43**(12), p 2978–2983
6. S. Miyazaki, H.Y. Kim, and H. Hosoda, Development and Characterization of Ni-Free Ti-Base Shape Memory and Superelastic Alloys, *Mater. Sci. Eng. A*, 2006, **438–440**, p 18–24
7. P. Laheurte, A. Eberhardt, and M.J. Philippe, Influence of the Microstructure on the Pseudoelasticity of a Metastable Beta Titanium Alloy, *Mater. Sci. Eng. A*, 2005, **396**(1–2), p 223–230
8. P. Laheurte, A. Eberhardt, M.J. Philippe, and L. Deblock, Improvement of Pseudoelasticity and Ductility of Beta III, Titanium Alloy—Application to Orthodontic Wires, *Eur. J. Orthod.*, 2007, **29**, p 8–13
9. W.F. Ho, C.P. Ju, and J.H. Chern Lin, Structure and Properties of Cast Binary Ti-Mo Alloys, *Biomaterials*, 1999, **20**, p 2115–2122
10. D. Kent, G. Wang, Z. Yu, and M.S. Dargusch, Pseudoelastic Behaviour of a Beta Ti-25Nb-3Zr-3Mo-2Sn Alloy, *Mater. Sci. Eng. A*, 2010, **527**, p 2246–2252
11. Y.L. Hao, S.J. Li, S.Y. Sun, C.Y. Zheng, and R. Yang, Elastic Deformation Behaviour of Ti-24Nb-4Zr-7.9Sn for Biomedical Applications, *Acta Biomater.*, 2007, **3**(2), p 277–286
12. A.J. Goldberg, R. Vanderby, Jr., and C.J. Burstone, Reduction in the Modulus of Elasticity in Orthodontic Wires, *J. Dent. Res.*, 1977, **56**(10), p 1227–1231
13. T.W. Duerig, Some Unsolved Aspects of Nitinol, *Mater. Sci. Eng. A*, 2006, **438–440**, p 69–74
14. C.V. Shastry and A.J. Goldberg, The Influence of Drawing Parameters on the Mechanical Properties of Two Beta-Titanium Alloys, *J. Dent. Res.*, 1983, **62**, p 1092–1097
15. Y.L. Hao, M. Niinomi, D. Kuroda, K. Fukunaga, Y.L. Zhou, R. Yang, and A. Suzuki, Young's Modulus and Mechanical Properties of Ti-29Nb-13Ta-4.6Zr in Relation to α″ Martensite, *Metall. Mater. Trans*, 2002, **33A**, p 3137–3144
16. M.J. Blackburn and J.A. Feeney, Stress-Induced Transformations in Ti-Mo Alloys, *J. Inst. Metals*, 1971, **99**(2), p 132–134
17. J.A. Roberson, S. Fujishiro, V.S. Arunachalam, and C.M. Sargent, Stress Induced Transformations in Beta III, Ti Alloy Single Crystals, *Metall. Trans.*, 1974, **5**, p 2317–2322
18. J.A. Roberson and A.M. Adair, Effects of Combined High and Low Temperature Deformation Processing of Beta III, Titanium, *Metall. Trans.*, 1972, **3**, p 1967–1972
19. H.Y. Kim, Y. Ikehara, J.I. Kim, H. Hosoda, and S. Miyazaki, Martensitic Transformation, Shape Memory Effect and Superelasticity of Ti-Nb Binary Alloys, *Acta Mater.*, 2006, **54**, p 2419–2429
20. H.Y. Kim, T. Sasaki, K. Okutsu, J.I. Kim, T. Inamura, H. Hosoda, and S. Miyazaki, Texture and Shape Memory Behavior of Ti-22Nb-6Ta Alloy, *Acta Mater.*, 2006, **54**, p 423–433

21. U.F. Kocks, C.N. Tomé, and H.R. Wenk, *Texture and Anisotropy*, Cambridge University Press, Cambridge, 2000
22. A. Bhattacharjee, S. Bhargava, V.K. Varma, S.V. Kamat, and A.K. Gogia, Effect of β Grain Size on Stress Induced Martensitic Transformation in β Solution Treated Ti-10V-2Fe-3Al Alloy, *Scripta Mater.*, 2005, **53**, p 195–200
23. T. Grosdidier, Y. Combres, E. Gautier, and M.J. Philippe, Effect of Microstructure Variations on the Formation of Deformation-Induced Martensite and Associated Tensile Properties in a β Metastable Ti Alloy, *Metall. Mater Trans.*, 2000, **31A**, p 1095–1106
24. E. Takashi, S. Watanabe, and S. Hanada, Superelastic Behavior in Nickel-Free Ti-Nb-Sn Alloys, *SMST-2003, Proceedings of the International Conference on Shape Memory and Superelastic Technologies*, A.R. Pelton and T. Duerig, Ed., SMST Society, Menlo Park, CA, 2003, p 91–99
25. S. Kajiwara, Roles of Dislocations and Grain Boundaries in Martensite Nucleation, *Metall. Trans.*, 1986, **17A**, p 1693–1702
26. L.C. Zhang, T. Zhou, M. Aindow, S.P. Alpay, and M.J. Blackburn, Nucleation of Stress-Induced Martensites in a Ti/Mo-Based Alloy, *J. Mater. Sci.*, 2005, **40**, p 2833–2836